Published in final edited form as:
Cancer Res. 2008 December 15; 68(24): 10051–10059. doi:10.1158/0008-5472.CAN-08-0786.

Cancer stem cells are enriched in the side-population cells in a mouse model of glioma

Molly A. Harris[1,2], **Hyuna Yang**[1], **Benjamin E. Low**[1], **Joydeep Mukherje**[3], **Abhijit Guha**[3], **Roderick T. Bronson**[4], **Leonard D. Shultz**[1], **Mark A. Israel**[5], and **Kyuson Yun**[1,*]

[1]The Jackson Laboratory, Bar Harbor, ME, 04609

[2]The Graduate School of Biomedical Sciences, University of Maine, Orono, ME 04469

[3]The Hospital for Sick Children, University of Toronto, Toronto, ON, Canada

[4]Harvard Medical School, Department of Pathology, Boston, MA, 02115

[5]Norris Cotton Cancer Center, Dartmouth-Hitchcock Medical Center, Lebanon, NH, 03756

Abstract

The recent identification of cancer stem cells (CSCs) in multiple human cancers provides a new inroad to understanding tumorigenesis at the cellular level. CSCs are defined by their characteristics of self-renewal, multipotentiality, and tumor initiation upon transplantation. By testing for these defining characteristics, we provide evidence for the existence of CSCs in a transgenic mouse model of glioma, *S100ß-verbB;Trp53*. In this glioma model, CSCs are enriched in the side-population (SP) cells. These SP cells have enhanced tumor-initiating capacity, self-renewal, and multipotentiality compared to non-SP cells from the same tumors. Furthermore, gene expression analysis comparing FACS-sorted cancer SP cells to non-SP cancer cells and normal neural SP cells identified 45 candidate genes that are differentially expressed in glioma stem cells. We validated the expression of two genes from this list (*S100a4* and *S100a6*) in primary mouse gliomas and human glioma samples. Analyses of xenografted human GBM (*glioblatoma multiforme*) cell lines and primary human glioma tissues show that S100A4 and S100A6 are expressed in a small subset of cancer cells and that their abundance is positively correlated to tumor grade. In conclusion, this study shows that CSCs exist in a mouse glioma model, suggesting that this model can be used to study the molecular and cellular characteristics of CSCs *in vivo* and to further test the cancer stem cell hypothesis.

Keywords

Cancer stem cells; tumor-initiating cells; glioma; GBM; glioblastoma; mouse models; side-population; SP cells

INTRODUCTION

The fundamental basis for the cancer stem cell hypothesis is the concept that there is a hierarchical organization of cells within a tumor and that only a subset of these cancer cells have the characteristics of stem cells (self-renewal and multipotentiality)(1, 2), and can also initiate a tumor when transplanted (3). In addition, cancer stem cells (CSCs) are thought to contribute to metastasis, therapy resistance, and recurrence (4). Emerging studies show that

*: To whom correspondence should be addressed. Kyuson.yun@jax.org, The Jackson Laboratory, 600 Main Street, mailbox 76, Bar Harbor, ME, 04609.

CSCs are indeed more resistant than other cancer cells to radiation- and chemo- therapies (5–9).

In human gliomas, early studies suggested that cancer-initiating cells are enriched in the CD133 + population (10). When CD133+ cells were injected orthotopically, as few as 100 of these cells could initiate a tumor while CD133− cells could not, even when 10,000 cells are injected (10). Furthermore, while CD133+ cells could give rise to both CD133+ and CD133− cells, CD133− cells could not give rise to CD133+ cells, indicating the more primitive differentiation status of CD133+ cells and the existence of cellular hierarchy in these glioma cells. However, more recent studies report that CD133− glioma cells can also initiate tumors and that there are tumor-initiating cells in gliomas that contain no CD133+ cells (11, 12). Together, these studies suggest that the CSC immunophenotype may vary among gliomas and that additional markers for CSCs are needed to better identify and study CSCs.

While CSCs have been identified in many human cancers (2), including brain, breast, colon, and hematological tumors, among others (10, 13–16), some have challenged the existence of rare cancer cells that have unique tumor-initiating ability. For example, Strasser and colleagues have challenged the existence of CSCs, based on the fact that the current definition of CSCs relies heavily on xenografting human cancer cells into immune-deficient mice and then asking whether a specific subpopulation is endowed with the ability to initiate a tumor; this approach may select for human cancer cells that can survive in mouse microenvironment but not necessarily for differential tumor-initiating capacity (17, 18). When Strasser and colleagues (17) transplanted cells from three different murine leukemia and lymphoma models into syngeneic mice, they observed that any 10 cancer cells (unsorted) could transfer the disease, arguing that cancer initiating cells are not rare when allogeneic transplantation is used. However, other studies have shown that there are identifiable, small subpopulation of leukemic cells that are more tumorigenic than other cancer cells using another mouse model of leukemia (19). These conflicting findings underscore the need to better define and understand CSCs and to further test whether CSCs exist in mouse models of human cancer, in particular in solid tumors.

To test whether CSCs exist in mouse brain tumors, we used a transgenic mouse model of glioma in which the S100ß-promoter drives the expression of the *verbB* gene (20). Approximately 60% of *S100ß-verbB* mice develop “spontaneous” gliomas by 12 months of age, and on the *Trp53*−/− (*p53*−/−) mutant background, nearly 100% of *S100ß-verbB;p53*−/− mice develop brain tumors by 4 months of age. Unlike transplanted neoplasms from xenografted human brain cancer cell lines, brain tumors in *S100ß-verbB;p53*−/− mice are highly infiltrative with extensive vascularization and necrosis (20) (Supplementary Figure 1a.b). In our colony of *S100ß-verbB;p53*−/− mice, most tumors observed are high-grade mixed gliomas, with histological features observed in malignant grade III and IV human gliomas. Hence, in light of the controversy that surrounds the existence of CSCs in mouse models of human cancer, we decided to test whether this mouse model of solid tumor contains cancer stem cell-like cells. Identification of mouse models that contain CSCs would enable exploitation of these models to study CSCs *in vivo*, including genetic manipulations to further test the CSC hypothesis, investigation of the influence of microenvironment on CSC behavior, large cohort studies using inbred strains of mice, and comparison of normal and cancer stem cells to determine the molecular differences between these cells from same organs.

Here, we report the existence of CSCs in a transgenic mouse brain tumor model. We show through prospective isolation and characterization of side-population (SP) cells that-tumor initiating cells are enriched in the SP cells in *S100ß-verbB;p53*−/− gliomas. Furthermore, SP cells show enhanced self-renewal and multipotentiality compared to non-SP cells from the same tumor, suggesting that CSCs are enriched within the SP cells. In addition, we identify a

gene signature that distinguishes brain cancer stem cells from non-stem cancer cells and normal neural stem cells. We selected two genes from this list with known expression in other aggressive human cancers (*S100A4* and *S100A6*) to test whether they are also expressed in human gliomas. Using primary human brain cancer tissues, we show that S100A4 and S100A6 are expressed in a subset of glioma cells. Furthermore, we show that there is a positive correlation between the glioma grade and percentages of S100A4− and S100A6-expressing cells in human samples, in particular in distinguishing *glioblastoma multiforme* (GBM) from lower grade gliomas.

MATERIALS AND METHODS

Cell cultures

Primary cells from *S100ß-verbB;p53*−/− or *S100ß-verbB;p53*+/− (maintained on an inbred C57BL/6J background) mouse brain tumors were isolated and cultured as tumorspheres in modified DME/F-12 supplemented with Neurocult Proliferation Supplement (Stemcell Technologies) or B27 (Invitrogen) and Penicillin/Streptomycin. Neurospheres were isolated from the SVZ region of C57BL6/J wildtype, *Trp53*−/−, and *S100ß-verbB;Trp53*−/− mice and cultured in the same medium supplemented with 20 ng/ml EGF and 10 ng/ml bFGF. Self-renewal assays were performed by plating dissociated single cells at 1cell/µl or 1 cell/10µl density and counting the number of spheres that formed after 6–7 days. Tumorspheres were induced to differentiate on poly-D-lysine/laminin-coated cover slips for 7 days using Neurocult Neural Differentiation Supplement (Stemcell Technologies): the components of this supplement are proprietary and are not available. Human brain cancer cell lines, U87, SF767, and HOG, were grown as monolayer cells in Dulbecco's Modification of Eagles' Medium (DMEM) with 10% fetal bovine serum with Penicillin/Streptomycin.

Immunohistochemistry

Standard immunofluorescence/immunohistochemical protocols were used. Mice with brain tumors were perfused and the whole brain was dissected, fixed, and embedded in OCT. Paraffin sections of human clinical GBM samples were obtained from Dr. Ab Guha, The Hospital for Sick Children, Toronto, and human glioma tissue arrays were purchased from Creative Biolabs. Human glioma S100A4+ and S100A6+ cells xenografted into NOD.CB17-*Prkdc*^{scid}/J immune-deficient mice were identified by immunofluorescence using an antibody against human specific nuclear antigen (HuNu, Millipore) or by establishing stable cells lines expressing GFP before transplantation. Because HuNu double staining could not be performed on clinical specimens, we relied on cell morphology to distinguish the human cancer cells from the reactive astrocytes (Supplementary Figure 2). The star morphology of the astrocytes was easily distinguished from the more round cancer cells. Only the rounded cells with strong immuno-reactivity to S100A4 or S100A6 were counted. Two representative fields from each of the clinical GBM samples were counted for S100A4+ and S100A6+ cells and averaged. Statistical significance of S100A4 and S100A6 expression in different glioma grades was calculated using the Tukey test.

Average percentages of positive cells expressing differentiation markers were measured by counting positive cells from five randomly selected fields on the coverslips containing differentiated neurosphere and tumorsphere cells.

Antibodies used for immunohistochemistry were: BCRP1 (Chemicon), SOX2 (Chemicon), GFAP (Chemicon), NG2 (Chemicon), MAP2 (Chemicon), HuNu (Millipore), and S100A6 & S100A4 (LabVision). Fluorescent sections were imaged using a Zeiss (Axiovert 200M) microscope with Apotome and analyzed with AxioVision software or a Leica SP5 confocal microscope with 100× objective, with a Z-stack projection.

FACS Analysis

Normal and tumor tissues and cultured cells were dissociated with Accutase (Invitrogen) digestion and mechanical trituration. Dissociated cells were stained using a standard FACS protocol. Antibodies used for FACS analyses were: anti PROM1/CD133 (eBioscience and Miltenyi) and BCPR1(Chemicon). For SP sorting, cells were incubated with Hoechst 33342 (Sigma) at a concentration of 5μg/ml at 37°C for 45 min. B6 bone marrow control cells were incubated for 90 min. Stained cells were rinsed and resuspended in ice-cold culture medium containing 2μg/ml Hoechst 33342 for FACS sorting.

Intracranial and subcutaneous injections

Tumor cells were injected subcutaneously into the flank or the brain of NOD-SCID immune-deficient mice or C57BL/6J syngeneic mice. For intracranial injections, cells were injected using a stereotaxic device (bregma: +2.5, −1.5, −3). The Animal Care and Use Committee at The Jackson Laboratory approved all animal procedures.

Real-Time RT-PCR analysis

RNA was treated with DNAse1 prior to cDNA conversion (using iScript from BioRad). Real-time PCR was performed using SYBR Green Supermix (BioRad) on a LightCycler PCR machine (Roche) or iQ5 PCR machine (Biorad). The primers used were: *S100a6*: 5'-TGAGCAAGAAGGAGCTGAAGGAGT-3' and 5'-TTCTGATCCTTGTTACGGTCCAGA-3', *S100a4*: 5'-TTTGAGGGCTGCCCAGATAAGGAA-3' and 5'-CACATGTGCGAAGAAGCCAGAGTA-3', and 18s: 5'GAGGGAGCCTGAGAAACGG-3' and 5'-GTCGGGAGTGGGTAATTTGC-3'.

Microarray data analysis

Three biological replicates of cancer1 (3447) and cancer2 (4346) were derived by transplanting primary tumorspheres into three recipient mice and isolating tumorsphere cells from resulting tumors. SP cells were FACS sorted from each tumorsphere line and hybridized onto separate Affymetrix GeneChips. Three neuroSP samples were derived from three individual control mice and hybridized separately. Three non-SP samples from cancer1 replicates were hybridized on three separate chips. Probe intensity data from 15 MOUSE430_2 Affymetrix GeneChip arrays were analyzed by R software. Affy probe was re-mapped by using custom CDF file (21) from Brain Array[1] to accommodate updated genome and transcription annotation. Perfect match intensities were normalized and summarized by the robust multi-array average (RMA) method. To identify differentially expressed genes between normal and cancer SP cells, cancer1 SP vs. neural SP, and cancer2 SP vs. neural SP, were compared. In both comparisons, Fs statistics, a modified F statistics with a shrinkage estimate of variance estimation, were calculated by MAANOVA (22). p-values were derived by 1000 permutations, and the false discovery rate (q-value) was calculated to correct for the multiple hypothesis-testing problem. Differentially expressed genes between cancer and neural SP cells were selected by two criteria: genes having < 0.05 q-value and > 2.6 (1.5 log2) fold change in both comparisons. Biological relationships among differentially expressed genes were studied using Ingenuity Systems[2] software. The GEO accession number for the microarray data is GPL1261.

[1]http://brainarray.mbni.med.umich.edu/Brainarray
[2]www.ingenuity.com

RESULTS

Neurospheres and tumorspheres display distinct cellular characteristics

CSCs in solid tumors have been shown to form tumorspheres, floating colonies of cells that resemble neurospheres formed by neural stem cells, in culture conditions that promote maintenance of stem cells. To identify distinguishing cellular and molecular phenotypes of tumorspheres and normal neurospheres, we isolated and characterized tumorspheres from tumor-bearing *S100ß-verbB;p53*−/− mice on a C57BL6/J (B6) background (Figure 1Aa) and neurospheres from asymptomatic *S100ß-verbB;p53*−/−, *p53*−/−, and wildtype *B6* control mice (Figure 1Ab). Tumorspheres (Figure 1Aa) grossly resembled neurospheres (Figure 1Ab) isolated from the subventricular zone (SVZ) of asymptomatic *S100ß-verbB;p53*−/− *p53*−/−, *and wildtype B6* mice, as well as previously described CSC-containing tumorspheres isolated from human tumors (23¯25). However, tumorspheres and neurospheres showed three distinguishable cellular characteristics: 1) neurospheres absolutely required the growth factor EGF (Epidermal Growth Factor) for growth, while tumorsphere cells grew in the absence of added growth factors or serum, demonstrating growth-factor independence (Figure 1B); 2) neurospheres were round, even-edged spheres, while tumorspheres were more loosely attached, exhibiting an uneven periphery, indicating reduced adherence (Figure 1Aa,b) neurosphere cells never initiated tumors when injected into immune-deficient or syngeneic mice while most tumorspheres formed tumors (Supplementary Table 1, $p<0.0001$).

Self-renewal, multipotentiality, and tumor-initiation of tumorspheres

To test for the frequency of tumorsphere-forming cells (cells with the ability to form floating colonies), we assessed the number of tumorspheres that form from freshly dissociated gliomas using a limiting dilution assay *in vitro*. Freshly dissociated glioma cells were plated at different doses and the number of spheres that form after 7 days in culture were measured. The frequency of tumorsphere-forming cells ranged between 1/333 and 1/500 cells in two independent tumors tested (Supplementary Table 2), suggesting that only a small subpopulation of tumor cells from *S100ß-verbB;p53* glioma could proliferate extensively to form colonies *in vitro*. To test whether these tumorspheres contained CSCs, we tested for three defining characteristics of CSCs: self-renewal, multipotentiality, and tumor-initiating capacity.

To test for self-renewal in these tumorsphere cultures, we dissociated established tumorspheres into single cells, plated them at a clonal density (1cell/µl), and counted the number of secondary spheres that formed after 7 days. Approximately 15–20% of the tumorsphere cells gave rise to secondary spheres (Figure 1C), indicating that the tumorspheres contain self-renewing stem cells. This capacity for self-renewal was maintained for more than 25 passages *in vitro*. To further test for the presence of stem cells, we isolated single cells and showed that they can self-renew and expand clonogenically in the absence of growth factors *in vitro* (Figure 1C).

To test multipotentiality, tumorsphere cells were cultured in NSC differentiation medium. Tumorsphere cells gave rise to cells expressing markers of all neural lineages, i.e; NG2+ (oligodendrocytes), GFAP+ (astrocytes), or MAP2+ (neurons), demonstrating multipotentiality (Figure 1D). The frequency of GFAP+ cells from tumorspheres (12.2%) was similar to that from neurospheres (7.6%) (p-value=0.139,). However, a significantly larger number of tumor cells expressed NG2 (66.7%) and MAP2 (63.2%) than did wildtype C57BL6/J neurosphere cells (16.3% and 18.9%, respectively; p-values = 0.0112 and 0.0005; Supplementary Figure 3) after 7 days in differentiation medium. This dysregulated differentiation gene expression pattern is consistent with abnormal differentiation in cancer cells (Figure 1Dd). Importantly, we observed identical cellular phenotypes (self-renewal and multipotentiality) in clonally-derived cell lines from single tumor cells (Figure 1C, Supplementary Table 1, and not shown).

To test tumor-initiating capacity, tumorsphere cells isolated from five independent tumors were injected either subcutaneously or orthotopically into the brain of either NOD.CB17-*Prkdc*^{scid}/J (NOD-SCID) immune-deficient mice or B6 syngeneic mice (Supplementary Table 1). In all cases, the transplanted neoplasms replicated the original tumor (Supplementary Figure 1A,B). Even injections of individual tumorspheres (containing approximately 100–200 cells) formed tumors in most cases, indicating that each tumorsphere contained at least one cancer-initiating cell (Supplementary Table 1). Histological analysis and molecular marker expression showed similar expression patterns between primary and transplanted, secondary tumors either in the flank or the brain (Supplementary Figure 1A, B). These tumors could be serially transferred through mice for more than 6 passages, demonstrating *in vivo* self-renewal ability. At each passage, tumorspheres were isolated and characterized, and their cellular characteristics with respect to growth rate and marker gene expression were similar to those of the original tumorsphere (not shown).

Cancer stem cells are enriched in the SP cells

To prospectively isolate CSCs, we examined expression patterns of candidate stem cell markers, including PROM1/CD133, BCRP1/ABCG2, CD44, c-Kit, and SOX2 in S100ß-verbB;p53 gliomas. SOX2 was expressed in the majority of cancer cells (Supplementary Figure 1Bb,c,d) suggesting that this is not a unique marker for the CSC subpopulation, since only a small fraction of the primary tumor cells could form tumorspheres (see above and Supplementary Table 2). This is in contrast to normal brain of B6 mice where high level SOX2 expression is restricted to the ependymal and subventricular zone where normal NSC are found, with a lower level of expression in scattered cells throughout the brain (Supplementary Figure 1Ba). ABCG2/BCRP1 was expressed in 2–5% of both the normal and tumorsphere cells (Supplementary Figure 1Ca,b), and we observed weak but consistent expression of CD133 in approximately 0.4–7% of tumorsphere cells, in contrast to expression of CD133 in approximately 6–36% cells in untransformed neurosphere cells (Supplementary Figure 1Cc,d). Interestingly, CD44 and c-Kit, stem cell markers in other tissues, were expressed in 60–80% of cells in both tumorsphere and neurosphere cultures (not shown), consistent with the report that CD44 is a marker of glial progenitors rather than stem cells (26). None of these markers were useful in prospective isolation of CSCs in our cultures (not shown).

We then turned to another common characteristic of CSCs: the ability to extrude chemicals through the function of multidrug resistance proteins (9). Others have shown that the SP is a cellular phenotype that arises from stem cells that extrude Hoechst 33342 dye; hence, most stem cells stain only weakly with this dye. This staining method has been used by many laboratories to isolate normal and cancer stem cells from multiple tissue types (27¯30). We stained *S100ßverbB;p53* tumorsphere cells with Hoechst 33342 dye and FACS sorted them for the SP and non-SP (Figure 2Ab). We then injected SP (0.15–1.2% of viable cells) and non-SP cells from the same tumorsphere cultures into NOD-SCID mice and compared their tumor-initiating abilities. As few as 50 SP cells initiated rapid tumor growth following transplantation in host mice, while 500 non-SP cells were required to give rise to tumors with similar frequency (Figure 2Ba, Supplementary Table 3, p-value = 0.0285). This suggests that tumor-initiating cells are enriched in the SP population.

To test whether SP cells also show other characteristics of CSCs, we examined their self-renewal ability and multipotentiality. We sorted SP and non-SP cells and cultured them at a clonal density. SP cells consistently gave rise to a larger number of secondary spheres than did non-SP cells (Figure 2Bb), indicating enhanced self-renewal of SP cells. In addition, we tested whether SP cells could give rise to both SP and non-SP cells, as would be expected of a stem cell population. When SP and non-SP cells were sorted and cultured, the sorted SP cells gave rise to approximately 12-fold more SP cells than did the sorted non-SP cells (Figure 2Ac,d, p-

value=0.045), consistent with a cellular hierarchy in which SP cells give rise to both SP and non-SP cells while non-SP cells do not (or rarely do). In addition, we consistently observed that secondary tumors contain SP+ cells (not shown), demonstrating *in vivo* self-renewal of SP cells. Together, these data indicate that CSCs are enriched in the SP cells in this cancer model and that SP cells can be used to examine the gene expression pattern of CSCs.

Gene expression analysis

Analysis of the molecular differences between CSCs, NSCs, and non-stem cancer cells may reveal novel markers for CSCs as well as molecular pathways that regulate CSCs. One of the major advantages of using inbred strains of mice is the nearly identical genetic background of different individuals of any given strain, which greatly facilitates comparative transcriptome analysis. To identify gene expression patterns that distinguish CSCs from NSCs, SP cells were isolated from both neurospheres (derived from *S100ß-verbB;p53*−/− and *p53*−/− brain) and tumorspheres (derived from *S100ß-verbB;p53*−/− gliomas). We used neurospheres from *p53* −/− background rather than wildtype B6 mice in this comparison since we wanted to identify genes that are differentially expressed in transformed cells from *S100ß-verbB;p53*−/− genotype and not just downstream targets of p53. Neurosphere cells from *S100ß-verbB;p53*−/− and *p53* −/− mice were tested both *in vitro* and *in vivo* to ensure that they were not transformed cells (i.e., that they were growth factor-dependent and non-tumorigenic) at the time of the microarray experiment (Figure 1B and Supplementary Table 1). SP and non-SP cells were directly sorted into a lysis buffer, and labeled probes were prepared from cDNAs and hybridized onto MOUSE430_2 Affymetrix GeneChip arrays. We found that 538 genes showed consistent expression differences between the six cancer SP (biological replicates from two independent tumors) and three independent neural SP cells (q-value <0.05 and Log2 change > 1.5) (Figure 3A). Of these, 345 genes were over-expressed and 193 genes were under-expressed in cancer-derived SP cells compared to neural SP cells (Supplementary Table 4). Unsupervised clustering of the data set using the 538 genes clearly segregated the cancer SP cells and neural SP cells (Figure 3Ac), as expected. Real-time RT-PCR validation with selected genes showed significant expression-level changes in components of the Wnt and Notch signaling pathways (*Dkk3*, *Wif1*, *Fzdb*, *Wnt7a*, *Wnt5a*, and *Hey2*), suggesting deregulation of these pathways that regulate NSCs in CSCs (Supplementary Table 5 and not shown).

To further filter the gene list for stem cell-relevant genes, we examined genes that are differentially expressed between cancer-initiating (SP) and non-initiating (non-SP) cells from the same tumorsphere cultures (Figure 3B). We first identified 244 genes that showed greater than a two-fold change in expression levels between cancer SP vs. cancer non-SP cells. This list included *Nanog*, *CD133*/*Prom1*, and *Myc*, genes associated with stem cells, validating our approach. To identify a gene list associated with glioma stem cells, we compared the two gene lists (cancer SP vs. neural SP and cancer SP vs. cancer non-SP cells). Forty-five genes were common to both gene lists (Figure 3Bb). We refer to this list of 45 genes as the brain CSC signature genes, as their expression patterns distinguish cancer SP cells from untransformed, neural SP and non-SP cancer cells. An unsupervised clustering analysis using this 45-gene list segregated cancer SP and non-SP samples (Figure 3Bc).

The 45-gene list (Table 1) includes many genes with known function in cancer, such as *Bgn*, *Mgp*, *Foxc2*, *Mia1*,*Cav1*, *S100a4*, and *S100a6*. We were particularly intrigued by the expression of *Foxc2*, *S100a4*/*Metastasin* and *S100a6*/*Calcyclin* Ca+ binding proteins, since they have been shown to mediate metastasis in other solid tumors (31¯33). We chose to further examine the expression of *S100a4* and *S100a6* in CSCs by RT-PCR and immunohistochemistry. Using quantitative RT-PCR from seven independent tumorspheres, we confirmed higher level of *S100a6* in tumorspheres compared to untransformed *S100ß-verbB;p53*+/− neurospheres (Figure 4A, p-value=0.0019). We observed a similar pattern with

S100a4 (not shown). In addition, RNA was extracted from SP and non-SP cells from two independent tumorspheres and the relative expression levels of *S100a6* and *S100a4* were measured by quantitative RT-PCR. Confirming our microarray results, both S100A6 and S100A4 were higher expressed in cancer SP cells than in non-SP cells from the same tumors (Figure 4B). Finally, on primary *S100ß-verbB;p53* glioma sections, only a small subset (2–4%) of cells expressed S100A4 and S100A6 proteins, consistent with their potential expression in CSCs (Figure 4C). Together, these results suggest that *S100a6* and *S100a4* are candidate markers for CSCs in gliomas.

S100A4 and S100A6 expression in human gliomas

To test whether *S100A4* and *S100A6* are expressed in human gliomas, we examined the expression patterns of S100A4 and S100A6 in clinical GBM samples, human brain tumor tissue arrays, and tumors derived from intracranial xenografts of human brain cancer cell lines (U87, SF767, and HOG cells) into NOD-SCID mice. In xenografted tumors, a subset of S100A4+ and S100A6+ cells co-expressed human-specific nuclear antigen (HuNu) (Figure 5Aa,b), indicating that these are transplanted cancer cells. These S100A4- and S100A6-expressing cells were often positioned in the periphery of the tumor or adjacent to blood vessels (not shown), the latter of which is a proposed niche for NSCs and glioma CSCs (34, 35). In clinical samples, strong S100A6 and S100A4 cytoplasmic staining was observed in scattered cancer cells throughout the tumors in all five GBM samples examined (Figure 5B,C). Significantly, in all tumors examined, many S100A6+ and S100A4+ cells were often observed adjacent to blood vessels (Figure 5B). The percentages of S100A4+ and S100A6+ cells varied among individual GBM samples (7.57–26.93%, Figure 5C) but the percentages of S100A4+ and S100A6+ cells in each of the samples were very similar (p-value=0.88).

It was previously proposed that the abundance of CSCs may correlate with the tumor grade (25). To examine whether *S100A4* and *S100A6* expression patterns correlate with tumor grade, we used a brain tumor tissue array containing normal brain tissue and gliomas from grade I through grade IV. As shown in Figure 5D, the percentages of *S100A4*-expressing cells in the different samples showed a positive correlation with tumor grade: normal tissue had no S100A4-positive cells, low grade gliomas had very few positive cells, and grade IV glioma samples had a large number of S100A4 expressing cells (>8% of total cells). In particular, S100A4 expression could clearly distinguish grade III and grade IV gliomas ($p<0.001$, Figure 5D and Supplementary Figure 2B).

DISCUSSION

In this report, we provide evidence for the first time that CSCs exist in a mouse model of glioma, rendering support for the cancer stem cell hypothesis. We present several lines of evidence that, in the *S100ß-verbB;p53* glioma mouse model, CSCs are enriched in the side-population (SP) cells. SP cells exhibit increased self-renewal ability, as demonstrated by an increased percentage of secondary sphere formation (Figure 2Bb) and generation of an increased number of SP cells upon culture (Figure 2A). Importantly, SP cells are more tumorigenic than non-SP cells (Figure 2B, Supplementary Table 3).

While earlier studies suggested that CSCs are enriched in the CD133+ population in human gliomas, more recent studies indicate that not all glioma stem cells are CD133+. While we were able to show that CSCs exist in *S100ß-verbB;p53* gliomas, we were not able to purify CSCs using PROM1/CD133 expression. Emerging studies are consistent with this in showing that CD133 is not an obligate marker for CSC in gliomas; some CD133− cells have been shown to be tumorigenic and have the potential to give rise to CD133+ cells (11, 12). We do not yet know whether the *S100ß-verbB:p53* model is representative of human gliomas in which CSCs

are CD133−, or whether CD133 antibodies that are available for mouse PROM1/CD133 do not have strong affinity for the glycosylated form of CD133 present on cancer cells.

Recent studies suggest molecular heterogeneity among CSCs (11, 12, 36, 37) suggesting that a single marker is unlikely to identify all CSCs, even within tumors of the same clinical grade from the same organ. We were unable to identify CSCs in S100ß-verbB;p53 gliomas using an immunophenotype (including ABCG2/BCRP1 or CD133 expression); hence, we used a cellular phenotype common to stem cells to sort for a specific subpopulation (side population) that enriches for CSCs. Staining for SP cells has been used to isolate bone marrow stem cells for many years (38), and recently this technique has been adopted by many researchers to enrich for normal and cancer stem cells from multiple tissue types (28, 29, 39). For example, Kondo et al. have shown that cancer-initiating cells of the C6 rat glioma cell line are enriched in the SP (28), and others have previously shown that normal NSCs neurosphere cultures are enriched in the SP (29), consistent with our observations (Figure 2Bb). However, some have reported increased cellular toxicity associated with Hoechst 33342 staining (a staining technique used to identify SP cells) questioning the usefulness of this technique to test for tumor initiation (40). In our hands, we observe equivalent levels of cell death in FACS-sorted SP and non-SP cells, most likely from the sorting itself, suggesting that selective cell death is not the major reason for differential tumorigenic potential we observe with SP cells.

While the molecular heterogeneity of SP cells is unknown in this tumor model, the relative enrichment (10–20 fold) of CSCs in the SP compared to non-SP tumorsphere cells (Figure 2Ba, Supplementary Table 3) is sufficient to enable identification of candidate genes that are differentially expressed in CSCs. By comparing purified populations of cells enriched in cancer stem vs. normal stem cells and in cancer stem vs. non-stem cancer cells, we identified a small number of genes whose expression distinguishes brain CSCs from neural stem and non-stem cancer cells. Notably, 23 of the 45 genes encode either secreted, membrane proteins or extracellular matrix components (Table 1), suggesting that a major distinguishing feature of the glioma SP cells we analyzed is their ability to interact with their microenvironment. The ability of cancer cells to establish themselves in a foreign cellular environment is an essential characteristic for successful metastasis and a defining characteristic of CSCs. Consistently, many genes on our list have known functions in mediating breast cancer metastasis. For example, a recent study has shown that FOXC2, a transcription factor on the list, is important in mediating breast cancer metastasis by regulating expression of genes that are involved in epithelial-mesenchymal transition (32). Consistently, we observed higher levels of *Snai2*, a transcription factor regulated by *Foxc2*, in tumorspheres than normal neurospheres (Supplementary Table 5). In addition, *S100a4*/*metastasin*/*Fsp1* was originally cloned as a gene that is differentially expressed in metastatic breast cancer cells, and it has been shown to have a causal role in mediating breast cancer metastasis (41, 42). Expression level of other genes on the list, such as S100A6, has been shown to correlate with pancreatic cancer prognosis (43) and colon cancer invasion/metastasis (33, 44). These observations suggest an intriguing possibility that the same molecular pathways that regulate metastasis in neoplasms outside of the nervous system may also be involved in gliomas.

While *S100A4* and *S100A6* expression and function have been reported in some cell populations in the brain, this has not been previously reported in brain cancer cells. In rodent brains, *S100a4* was reported to be expressed in a subset of white matter glial cells and reactive astrocytes after injury (45). While we do observe S100A4+/GFAP+ reactive astrocytes in transplant-recipient mouse brains, we were able to specifically identify S100A4+ cancer cells, as the astrocytes were distinguishable from cancer cells by their normal cellular morphology and GFAP expression. (Supplementary Figure 2A, and not shown). Similarly, *S100a6*/*Calcyclin* was reported to be expressed in the subventricular zone and ependymal layer of normal brain (46), where *Prom1*/*CD133*, *Sox2*, and *Nestin* (markers of NSCs) are also

expressed. In human glioma samples, we observed that: 1) only a small subset of cancer cells express S100A4 and S100A6 (Figures 4C, 5), and 2) many S100A4 and S100A6+ cells are associated with the stem cell niche in the brain, the endothelium (34, 35) (Figure 5B). In support of a link between these genes and CSCs, S100A4 and S100A6 expression has been reported to be associated with other stem cells (47, 48). We are currently testing the hypothesis that S100A4 and S100A6 may be new markers for CSCs by prospective sorting and transplantation of S100A4+ or S100A6+ cells in *S100ß-verbB;p53* gliomas and by examining co-expression of S100A4 and S100A6 with known stem cell markers in human gliomas.

Regardless of whether S100A4 and S100A6 expression identifies human glioma stem cells, our data indicate that the abundance of S100A4+ and S100A6+ cells in clinical glioma samples distinguishes undifferentiated, aggressive GBMs (grade IV) from grade III gliomas ($p<0.001$, Figure 5D). Using 19 different primary human samples (triplicate plugs from each sample), we show that only grade IV GBM samples contain >8% S100A4+ cells. While a study involving a larger sample size is needed to further validate this finding, our pilot study provides a promising indication that the genes we identified by studying mouse gliomas may be useful in studying human gliomas. Considering the significant differences in the clinical outcomes and treatment regiments for GBM patients compared to those for patients with lower grade gliomas, a retrospective and/or a prospective study involving a larger set of samples to validate the use of S100A4 and S100A6 as biomarkers for GBMs and CSCs is a promising line of investigation.

While this manuscript was in revision, another group reported identification of a population of tumor-initiating cells in a mouse model of breast cancer (49), supporting the existence of CSC-like cells in mouse models of solid tumors. Together with other studies using mouse models (19, 50), our study provides growing support for the cancer stem cell hypothesis. Therefore, in selected tumor models, murine cancer cells are organized in a hierarchy consistent with the cancer stem cell hypothesis, and that the understanding of the biology of CSCs (cell of origin, therapy resistance, and stem-niche interaction, for example) can be significantly advanced using these *in vivo* models.

Supplementary Material

Refer to Web version on PubMed Central for supplementary material.

Acknowledgments

We thank Eric Dufour, Ted Duffy, Will Schott, Sonya Kamdar, Weidong Zhang, and Karen Hammond for their assistance with this project. We also thank Kevin Mills, Shaoguong Li, Susan Ackerman, Gary Churchill, Barbara Tennent, and Barbara Knowles for critical reading of this manuscript, The Jackson Laboratory's Multimedia Services for their assistance with graphic arts, and all members of the Yun laboratory for their input and help throughout this project.

Financial Support: This project was funded in part by a Betz Foundation grant to MI, the TJL Cancer Center Support Grant CA034196, and the Oligodendroglioma Grant from the National Brain Tumor Foundation to KY.

REFERENCES

1. Bonnet D, Dick JE. Human acute myeloid leukemia is organized as a hierarchy that originates from a primitive hematopoietic cell. Nat Med 1997;3:730–7. [PubMed: 9212098]
2. Dalerba P, Cho RW, Clarke MF. Cancer stem cells: models and concepts. Annu Rev Med 2007;58:267–84. [PubMed: 17002552]
3. Wicha MS, Liu S, Dontu G. Cancer stem cells: an old idea--a paradigm shift. Cancer Res 2006;66:1883–90. discussion 95–6. [PubMed: 16488983]

4. Zhang M, Rosen JM. Stem cells in the etiology and treatment of cancer. Curr Opin Genet Dev 2006;16:60–4. [PubMed: 16377171]
5. Ma S, Lee TK, Zheng BJ, Chan KW, Guan XY. CD133(+) HCC cancer stem cells confer chemoresistance by preferential expression of the Akt/PKB survival pathway. Oncogene. 2007
6. Bao S, Wu Q, McLendon RE, et al. Glioma stem cells promote radioresistance by preferential activation of the DNA damage response. Nature 2006;444:756–60. [PubMed: 17051156]
7. Liu G, Yuan X, Zeng Z, et al. Analysis of gene expression and chemoresistance of CD133+ cancer stem cells in glioblastoma. Mol Cancer 2006;5:67. [PubMed: 17140455]
8. Rich JN. Cancer stem cells in radiation resistance. Cancer Res 2007;67:8980–4. [PubMed: 17908997]
9. Dean M, Fojo T, Bates S. Tumour stem cells and drug resistance. Nat Rev Cancer 2005;5:275–84. [PubMed: 15803154]
10. Singh SK, Hawkins C, Clarke ID, et al. Identification of human brain tumour initiating cells. Nature 2004;432:396–401. [PubMed: 15549107]
11. Beier D, Hau P, Proescholdt M, et al. CD133(+) and CD133(−) glioblastoma-derived cancer stem cells show differential growth characteristics and molecular profiles. Cancer Res 2007;67:4010–5. [PubMed: 17483311]
12. Wang J, Sakariassen PO, Tsinkalovsky O, et al. CD133 negative glioma cells form tumors in nude rats and give rise to CD133 positive cells. Int J Cancer 2008;122:761–8. [PubMed: 17955491]
13. Prince ME, Sivanandan R, Kaczorowski A, et al. Identification of a subpopulation of cells with cancer stem cell properties in head and neck squamous cell carcinoma. Proc Natl Acad Sci U S A 2007;104:973–8. [PubMed: 17210912]
14. O'Brien CA, Pollett A, Gallinger S, Dick JE. A human colon cancer cell capable of initiating tumour growth in immunodeficient mice. Nature 2007;445:106–10. [PubMed: 17122772]
15. Al-Hajj M, Wicha MS, Benito-Hernandez A, Morrison SJ, Clarke MF. Prospective identification of tumorigenic breast cancer cells. Proc Natl Acad Sci U S A 2003;100:3983–8. [PubMed: 12629218]
16. Dalerba P, Dylla SJ, Park IK, et al. Phenotypic characterization of human colorectal cancer stem cells. Proc Natl Acad Sci U S A 2007;104:10158–63. [PubMed: 17548814]
17. Kelly PN, Dakic A, Adams JM, Nutt SL, Strasser A. Tumor growth need not be driven by rare cancer stem cells. Science 2007;317:337. [PubMed: 17641192]
18. Hill RP. Identifying cancer stem cells in solid tumors: case not proven. Cancer Res 2006;66:1891–5. discussion 0. [PubMed: 16488984]
19. Yilmaz OH, Valdez R, Theisen BK, et al. Pten dependence distinguishes haematopoietic stem cells from leukaemia-initiating cells. Nature 2006;441:475–82. [PubMed: 16598206]
20. Weiss WA, Burns MJ, Hackett C, et al. Genetic determinants of malignancy in a mouse model for oligodendroglioma. Cancer Res 2003;63:1589–95. [PubMed: 12670909]
21. Dai M, Wang P, Boyd AD, et al. Evolving gene/transcript definitions significantly alter the interpretation of GeneChip data. Nucleic Acids Res 2005;33:e175. [PubMed: 16284200]
22. Wu, H.; Kerr, K.; Churchill, GA. The Analysis of Gene Expression Data: An Overview of Methods and Software. 2003. MAANOVA: a software package for the analysis of spotted cDNA microarray experiments; p. 313-431.
23. Galli R, Binda E, Orfanelli U, et al. Isolation and characterization of tumorigenic, stem-like neural precursors from human glioblastoma. Cancer Res 2004;64:7011–21. [PubMed: 15466194]
24. Hemmati HD, Nakano I, Lazareff JA, et al. Cancerous stem cells can arise from pediatric brain tumors. Proc Natl Acad Sci U S A 2003;100:15178–83. [PubMed: 14645703]
25. Singh SK, Clarke ID, Terasaki M, et al. Identification of a cancer stem cell in human brain tumors. Cancer Res 2003;63:5821–8. [PubMed: 14522905]
26. Liu Y, Han SS, Wu Y, et al. CD44 expression identifies astrocyte-restricted precursor cells. Dev Biol 2004;276:31–46. [PubMed: 15531362]
27. Patrawala L, Calhoun T, Schneider-Broussard R, Zhou J, Claypool K, Tang DG. Side population is enriched in tumorigenic, stem-like cancer cells, whereas ABCG2+ and ABCG2− cancer cells are similarly tumorigenic. Cancer Res 2005;65:6207–19. [PubMed: 16024622]
28. Kondo T, Setoguchi T, Taga T. Persistence of a small subpopulation of cancer stem-like cells in the C6 glioma cell line. Proc Natl Acad Sci U S A 2004;101:781–6. [PubMed: 14711994]

29. Kim M, Morshead CM. Distinct populations of forebrain neural stem and progenitor cells can be isolated using side-population analysis. J Neurosci 2003;23:10703–9. [PubMed: 14627655]
30. Goodell MA, McKinney-Freeman S, Camargo FD. Isolation and characterization of side population cells. Methods Mol Biol 2005;290:343–52. [PubMed: 15361673]
31. Garrett SC, Varney KM, Weber DJ, Bresnick AR. S100A4, a mediator of metastasis. J Biol Chem 2006;281:677–80. [PubMed: 16243835]
32. Mani SA, Yang J, Brooks M, et al. Mesenchyme Forkhead 1 (FOXC2) plays a key role in metastasis and is associated with aggressive basal-like breast cancers. Proc Natl Acad Sci U S A 2007;104:10069–74. [PubMed: 17537911]
33. Komatsu K, Kobune-Fujiwara Y, Andoh A, et al. Increased expression of S100A6 at the invading fronts of the primary lesion and liver metastasis in patients with colorectal adenocarcinoma. Br J Cancer 2000;83:769–74. [PubMed: 10952782]
34. Calabrese C, Poppleton H, Kocak M, et al. A perivascular niche for brain tumor stem cells. Cancer Cell 2007;11:69–82. [PubMed: 17222791]
35. Shen Q, Goderie SK, Jin L, et al. Endothelial cells stimulate self-renewal and expand neurogenesis of neural stem cells. Science 2004;304:1338–40. [PubMed: 15060285]
36. Hermann PC, Huber SL, Herrler T, et al. Distinct populations of cancer stem cells determine tumor growth and metastatic activity in human pancreatic cancer. Cell Stem Cell 2007;1:313–23. [PubMed: 18371365]
37. le Viseur C, Hotfilder M, Bomken S, et al. In childhood acute lymphoblastic leukemia, blasts at different stages of immunophenotypic maturation have stem cell properties. Cancer Cell 2008;14:47–58. [PubMed: 18598943]
38. Goodell MA, Brose K, Paradis G, Conner AS, Mulligan RC. Isolation and functional properties of murine hematopoietic stem cells that are replicating in vivo. J Exp Med 1996;183:1797–806. [PubMed: 8666936]
39. Szotek PP, Pieretti-Vanmarcke R, Masiakos PT, et al. Ovarian cancer side population defines cells with stem cell-like characteristics and Mullerian Inhibiting Substance responsiveness. Proc Natl Acad Sci U S A 2006;103:11154–9. [PubMed: 16849428]
40. Siemann DW, Keng PC. Cell cycle specific toxicity of the Hoechst 33342 stain in untreated or irradiated murine tumor cells. Cancer Res 1986;46:3556–9. [PubMed: 3708586]
41. Davies MP, Rudland PS, Robertson L, Parry EW, Jolicoeur P, Barraclough R. Expression of the calcium-binding protein S100A4 (p9Ka) in MMTV-neu transgenic mice induces metastasis of mammary tumours. Oncogene 1996;13:1631–7. [PubMed: 8895508]
42. Grum-Schwensen B, Klingelhofer J, Berg CH, et al. Suppression of tumor development and metastasis formation in mice lacking the S100A4(mts1) gene. Cancer Res 2005;65:3772–80. [PubMed: 15867373]
43. Ohuchida K, Mizumoto K, Yu J, et al. S100A6 is increased in a stepwise manner during pancreatic carcinogenesis: clinical value of expression analysis in 98 pancreatic juice samples. Cancer Epidemiol Biomarkers Prev 2007;16:649–54. [PubMed: 17416753]
44. Komatsu K, Murata K, Kameyama M, et al. Expression of S100A6 and S100A4 in matched samples of human colorectal mucosa, primary colorectal adenocarcinomas and liver metastases. Oncology 2002;63:192–200. [PubMed: 12239456]
45. Kozlova EN, Lukanidin E. Metastasis-associated mts1 (S100A4) protein is selectively expressed in white matter astrocytes and is up-regulated after peripheral nerve or dorsal root injury. Glia 1999;27:249–58. [PubMed: 10457371]
46. Yamashita N, Ilg EC, Schafer BW, Heizmann CW, Kosaka T. Distribution of a specific calcium-binding protein of the S100 protein family, S100A6 (calcyclin), in subpopulations of neurons and glial cells of the adult rat nervous system. The Journal of comparative neurology 1999;404:235–57. [PubMed: 9934997]
47. Tumbar T, Guasch G, Greco V, et al. Defining the epithelial stem cell niche in skin. Science 2004;303:359–63. [PubMed: 14671312]
48. Morris RJ, Liu Y, Marles L, et al. Capturing and profiling adult hair follicle stem cells. Nat Biotechnol 2004;22:411–7. [PubMed: 15024388]

49. Zhang M, Behbod F, Atkinson RL, et al. Identification of tumor-initiating cells in a p53-null mouse model of breast cancer. Cancer Res 2008;68:4674–82. [PubMed: 18559513]

50. Cho RW, Wang X, Diehn M, et al. Isolation and Molecular Characterization of Cancer Stem Cells in MMTV-Wnt-1 Murine Breast Tumors. Stem Cells 2008:364–71. [PubMed: 17975224]

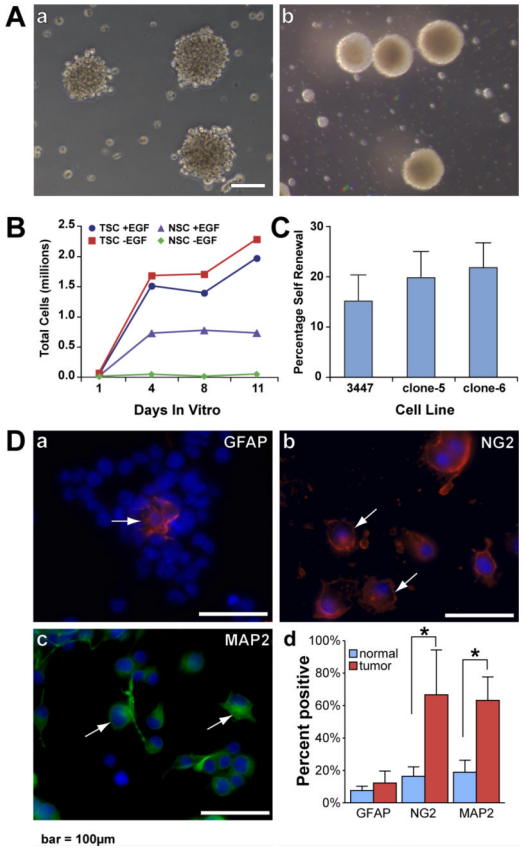

Figure 1. Isolation and characterization of tumorspheres from *S100β-verbB;p53−/−* gliomas

(A) (a) Tumorspheres from *S100β-verbB;p53−/−* gliomas grown in serum-free medium without added growth factors. (b) Neurospheres isolated from the subventricular zone of asymptomatic *S100β-verbB;p53−/−* mice, grown in serum-free medium containing bFGF and EGF. (B) Growth-curve comparing neurospheres and tumorspheres grown in the presence or absence of EGF (plated 1E5 cells on day 0). (C) Self-renewal assay of a parental (3447) and two clonally derived tumorsphere cell lines (measured as percentage of single cells giving rise to secondary spheres when plated at 1 cell/μl). (D) Dissociated tumorsphere cells plated on poly-D-lysine/laminin-coated coverslips, after 7 days in differentiation medium, stained with: (a) GFAP: astrocyte marker in red (14.1±7.33%); (b) NG2: early oligodendrocyte marker in red (70.6±27.6%); and (c) MAP2: neuronal marker in green (66.3±14.42%). Arrows indicate positively stained cells. All nuclei are marked in blue by DAPI staining. (d) Quantitation of cells expressing differentiation markers are compared between neurospheres (shown in Supplementary Figure 3) and tumorspheres. Five fields on each coverslip were randomly selected, and positive and total cells were counted. normal= neurosphere cells from wildtype C57BL6/J; tumor= tumorsphere cells from a *S100β-verbB;p53−/−* mouse. Asterisks indicate statistically significant differences, calculated using the Welsh two sample t-test).
Scale bar = 100μm.

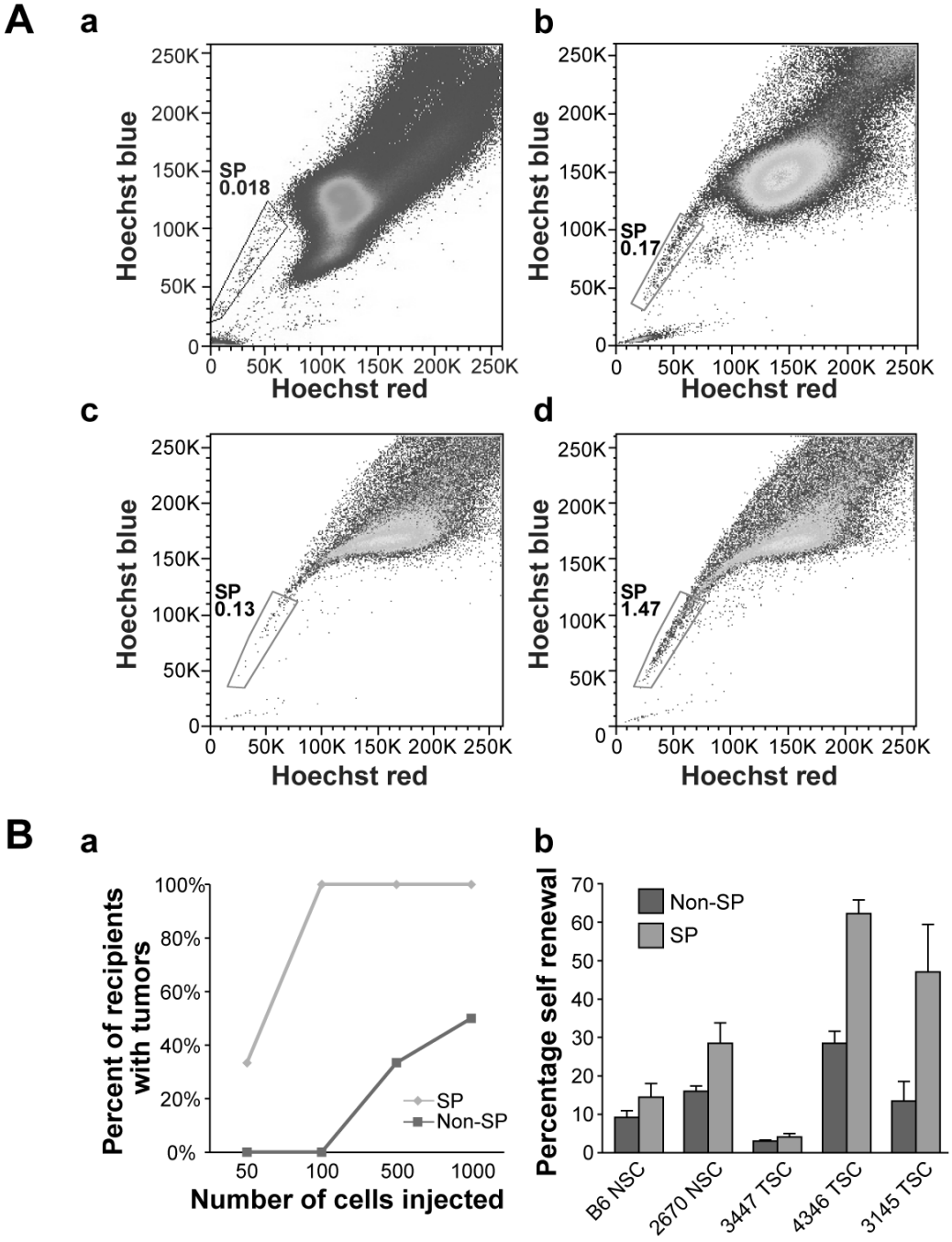

Figure 2. Isolation and characterization of cancer SP cells

(A) Hoechst 33342 staining of (a) bone marrow control cells and (b) tumorsphere cells showing SP cells in gated areas. Tumor cells were sorted into SP and non-SP cells and cultured: (c) Non-SP cells give rise to 0.13% SP, while (d) SP cells give rise to 1.47% (approximately 12-fold more) SP cells after two passages in culture. Hoechst stain and FACS sort scans were performed on 3 independent primary tumorsphere lines with similar results (p-value = 0.045, paired t-test). (B) (a) Percentage of recipient mice giving rise to tumors. Graph is a summary of four independent FACS sorts and injections comparing SP and non-SP (p-value =0.0285, logistic regression was used for statistical analysis). Two to 12 mice were injected with each cell dose (see Supplementary Table 3 for details). (b) Self-renewal assay of two neurosphere

lines and three tumorsphere lines, comparing the percentages of secondary sphere formation by SP and non-SP cells (p-value=0.0471, paired t-test).

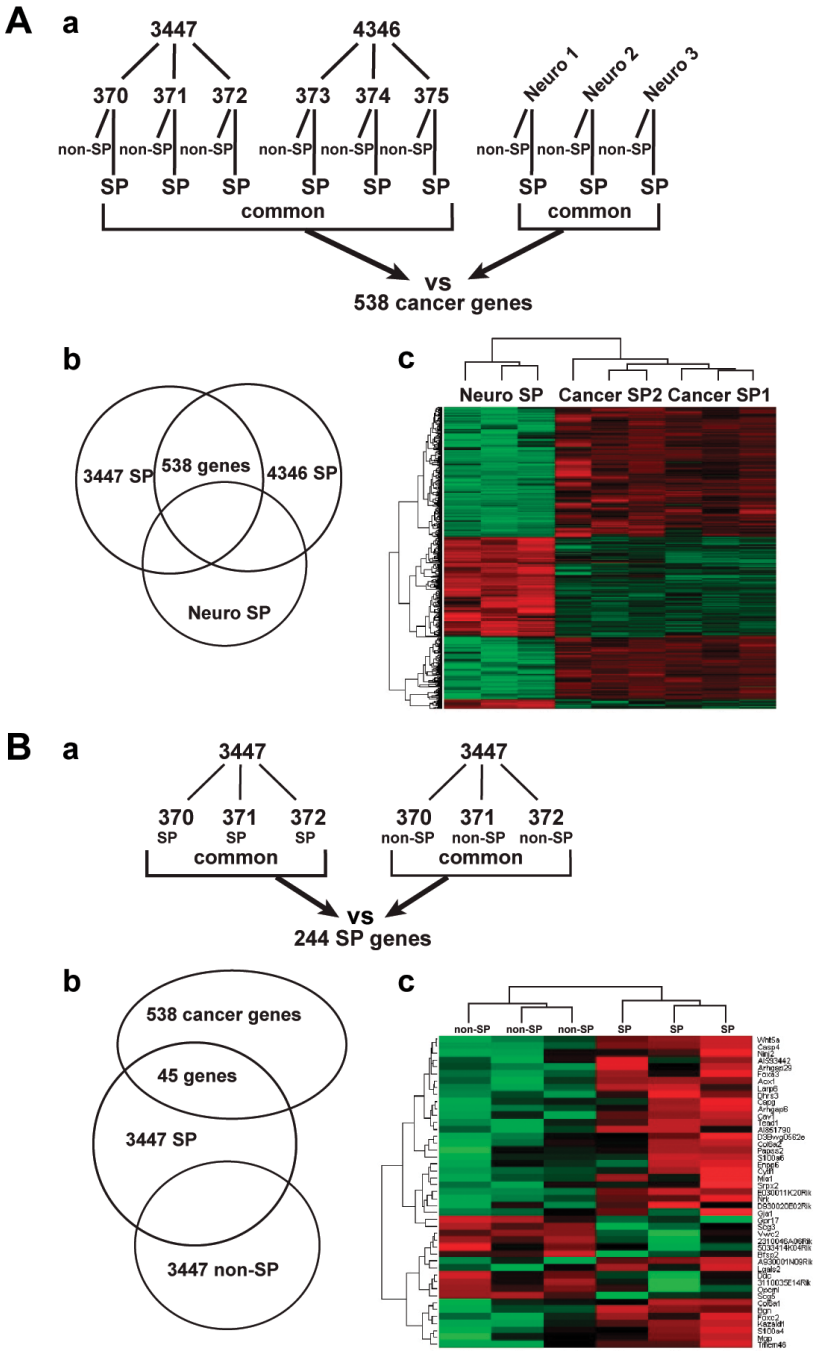

Figure 3. Microarray analysis of SP sorted normal and cancer cells

(A) (a) SP cells were purified from six tumorsphere cultures (biological triplicates derived from transplanting two independent primary tumors) and three independent neurosphere cultures from two *p53−/−* mice and one *S100β-verbB;p53−/−* mouse. (b) 538 differentially expressed genes were identified by comparing six cancer SP and three neural SP cells with q-value <0.05 and log2 change >1.5 (“cancer genes”). (c) Unsupervised clustering of the 538 genes segregates cancer SP and neural SP samples (B) (a) Gene expression comparison between cancer SP and non-SP cells from the same tumor identified 244 “SP genes” with at least a 2-fold change in expression levels. (b) The “SP gene” list was compared to the “cancer gene” list to identify a common subset of genes. The resulting common gene list consists of 45 genes (see Table 1),

which segregates SP and non-SP samples when unsupervised clustering analysis was used, shown in (c). Red color indicates higher level of expression in the heat-maps in (Ac) and (Bc).

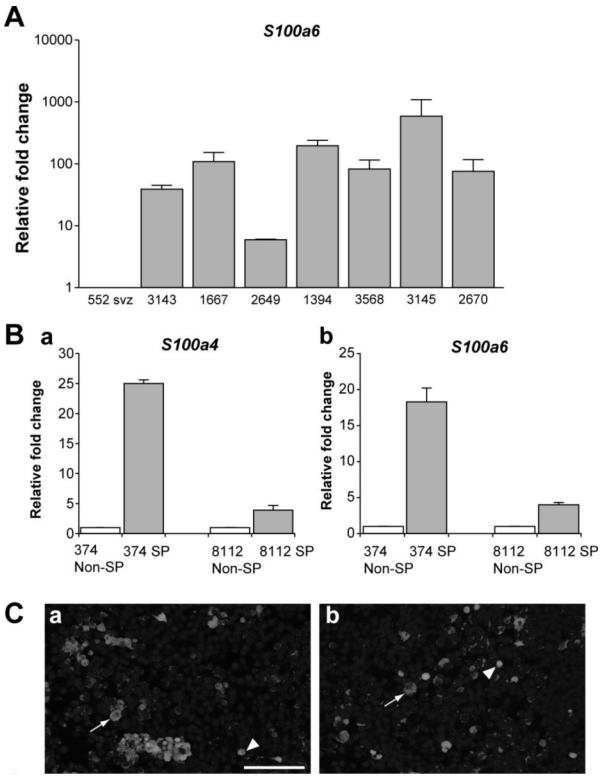

Figure 4. *S100a4* and *S100a6* expression levels are elevated in cancer SP cells

(A) Real-time RT-PCR analysis using RNA from two untransformed neurospheres from *S100β-verbB;p53*+/− mice and seven independent tumorsphere lines from *S100β-verbB;p53* −/− or *S100β-verbB;p53*+/− gliomas. Relative *S100a6* expression levels in tumorspheres are compared to the untransformed neurosphere levels (p-value=0.0019, Welsh two sample t-test). (B) Relative *S100a4* (a) and *S100a6* (b) expression levels between SP and non-SP cells, with the non-SP level set at 1. Analyzed with two independent tumorsphere lines and repeated with at least three technical replicates. All samples in A and B were normalized to internal 18S levels. (C) Immunofluorescence analysis of primary mouse gliomas using an antibody against S100A6 (a) and S100A4 (b). Both cytoplasmic (arrow) and nuclear (arrowhead) staining was observed for both antibodies. All nuclei are marked in blue by DAPI staining. Scale bar = 100μm.

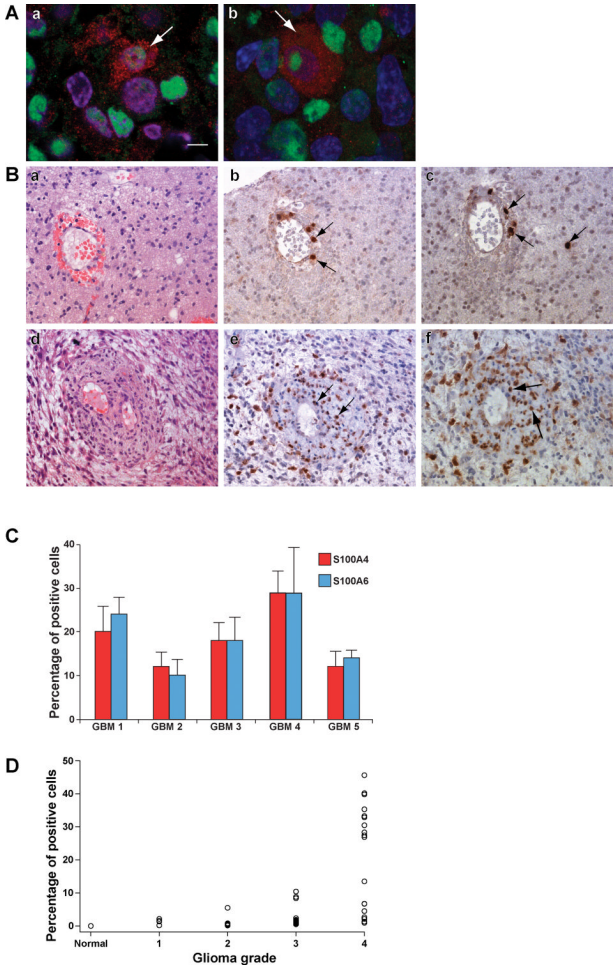

Figure 5. S100A6 and S100A4 expression in human brain tumor tissues

(A) Immunofluorescence analysis of U87 (a human GBM cell line) xenografted tumor, using an antibody against S100A4 (a) and S100A6 (b), both in red, and human nuclear antigen (HuNu) antibody in green, DAPI in blue (a,b). (B) Primary human GBM samples; GBM2 (a-c) and GBM4 (d-f). H&E staining (a,d) and adjacent sections stained with S100A4 (b,e) and S100A6 (c,f). Arrows indicate S100A4+ or S100A6+ human cells. (C) Average percentage of S100A4+ and S100A6+ cells in five independent human GBM tissues (p=0.881, Welsh two sample t-test). Averages were calculated from counts of three randomly chosen fields from each tumor. (D) Tissue arrays containing triplicates of normal cerebrum tissue and 19 independent human gliomas of varying grades were stained with S100A4 antibody. Graph represents the average percentage of S100A4+ cells in each sample (averaged from two random fields) from 16 tumors (five grade IV, six grade III, two grade II, and one grade I) and three normal tissue samples. Expression of S100A4 was significantly higher in grade IV compared to grade III gliomas (p-value<0.001, Tukey test), as well as between grade IV gliomas and grade II gliomas, grade I gliomas, and normal tissue samples. Ttwo independent neuropathologists determined the tumor grades on the tissue array, using the WHO grading scheme. Scale bar= 100μm

Table 1

45-brain cancer stem cell signature genes Average fold change between normal SP and cancer SP from the microarray analysis are indicated in parentheses. Selected genes were validated with RT-PCR (in bold).

Category	N=45	Genes
Extracellular	9	**Mgp**(99.5×), **Bgn**(102×), Kazald1(19×), **Col6a1**(15.7×), Scg5 (8.5×), Col6a2(14.6×), Vwc2(4.2×), Mia1(5.9×), **Scg3** (0.2×)
Membrane/cell signaling	12	Tmem46(6.5×), Opcml (6.2×), Ninj2(8.5×), Enpp6 (6.3×), **Cav1**(15.7×), **S100a6**(31.5×), **S100a4**(14.7×), Gpr17(8.7×), D930020E02Rik (0.1×), **Gja1**(0.1×), 5033414K04Rik (0.2×), Kcna4 (12.9×)
secreted	3	**Cytl1**(16.1×), AI851790 (0.2×), Wnt5a (0.2×),
DNA/RNA binding	5	**Foxc2**(32.6×), Foxa3(10.6×), **A930001N09Rik**(4.5×), Larp6 (5.4×), Tead1 (0.3×)
Kinase/phosphatase/GTPase	4	Papss2 (39.7×), Arhgap6 (13.2), D3Bwg0562e (6.2×), Arhgap29 (0.3×),
Apoptosis	1	Casp4(12.4×)
Novel genes	4	3110035E14Rik (12.1×), 2310046A06Rik (8.2×), E030011K20Rik (5×), Ai593442 (0.1×)
others	7	Ddc(20.4×), Lgals2 (11.7×), Capg(15×), Srpx2 (7.4×), Dhrs3 (4.1×), Bfsp2 (15.1×), Aox1 (0.3×)